ELSEVIER

Journal of Nuclear Materials 290–293 (2001) 793–797

journal of nuclear materials

www.elsevier.nl/locate/jnucmat

Numerical simulation of hydrogen molecular dissociation and the effects to Hα profiles in low temperature plasmas

Bingjia Xiao [a,*,1], Shinichiro Kado [b], Kazuki Kobayashi [a], Satoru Tanaka [a]

[a] *Department of Quantum Engineering and Systems Science, Graduate School of Engineering, The University of Tokyo, 7-3-1 Hongo, Bunkyo-ku, Tokyo, Japan*

[b] *High Temperature Plasma Centre, The University of Tokyo, 2-16-11 Yayoi, Bunkyo-ku, Tokyo, Japan*

Abstract

Hydrogen molecules may have considerably high density in edge regions of fusion devices so that clarifying their behavior in edge plasmas is very important in understanding the phenomena near plasma facing materials. This paper evaluated the energy distribution of the dissociated products of H_2 due to the electron induced excitation to the repulsive state $b^3\Sigma_u$ and the excitation to $a^3\Sigma_u$ followed by the radiative decay to the repulsive state $b^3\Sigma_u$ under the framework of Gryzinski approximation [M. Gryzinski, Phys. Rev. 138 (2A) (1965) A305, A322, A366]. The vibrational populations of H_2 were considered in the calculation. The results show that the dissociated atoms from these channels are highly distributed in the low energy range (<1 eV) while there is no significant distribution in the high energy range (>3 eV), when H_2 molecules are vibrationally excited. The discussions were made on the influences to Hα profiles in the low temperature plasmas [S. Tanaka, B.J. Xiao, K., Kobayashi , M. Morita, Plasma Phys. Control Fus. 42 (2000) 1091]. It is shown that the contribution of the low energy atoms in ground state may not be the only contributions of the low energy component in the observed Hα especially when $H_2(X^1\Sigma_g^+) + e \rightarrow H_2(1s\sigma, nl\lambda|^1\Lambda) \rightarrow e + H(1s) + H(2s)$ reaction has considerable reaction rates in the electron temperature around 10 eV.

Keywords: Hydrogen molecules; Dissociation; Energy distribution; Vibrational excitation; FCFRKR code

1. Introduction

Hydrogen molecules are desorbed from plasma facing materials when hydrogen ions or atoms impinge on the targets, and also, they can be introduced by fueling or puffing into edge plasmas. In the near wall region, molecules can occupy large fraction of neutral particles especially when the detachment or high recycling scenarios are selected for the divertor operation. In these cases, the behavior of the molecules will have large influences on both the main and the edge plasma properties and behaviors.

One of the important issues is the energy distribution of the dissociated products of hydrogen molecules. A very low energy component was observed in the edge plasma region in the TEXTOR experiments [3]. The energy distribution of the dissociated products as well as the electron induced reaction rates is strongly dependent on the vibrational population of the molecules. In Section 2, we report our calculation of the energy distribution of the dissociated atoms under the framework of Gryzinski approximation. We thus make a discussion on its influence to the $H\alpha$ profile near the plasma facing material surfaces in Section 3.

2. The energy distribution of the dissociated atoms

The dissociation of molecules can take place via various pathways among which the reaction

* Tel.: +81-358 416 968; fax: +81-358 418 625.

E-mail addresses: bjxiao@flanker.q.t.u-tokyo.ac.jp, bjxiao@mail.ipp.ac.cn (B. Xiao).

[1] Permanent address: Institute of Plasma Physics, Chinese Academy of Sciences, P.O. Box 1126, Hefei, Anhui 230031, China

0022-3115/01/$ - see front matter
PII: S0022-3115(00)00465-7

$$e + H_2(X) \rightarrow e + H2(a^3\Sigma_g, b^3\Sigma_u, c^3\Pi_u) \rightarrow e + H(1s) + H(1s) \qquad \text{(reaction A)}$$

is the dominant process for the molecule dissociation in the electron energy around 10 eV.

We firstly discuss the excitation to the repulsive state $b^3\Sigma_u$ (referred to X-b hereafter). We start from the cross-sections. In the past 30 years, there were many calculations and there were some experimental measurement as well being performed for the cross-sections of hydrogen molecular dissociation, i.e. [4,5] and the referenced work therein. However, the complete data sets dealing with the vibrationally excited H_2 have not been available. Following Cacciatore [6,7] and Celiberto [8], we adopt the Gryzinski method [1] and its extension to molecules [9] in the calculation of the cross-sections. The excitation to a triplet state is a spin change process, which is optically forbidden. The collision can occur when a mobile orbital electron receives enough energy to be ejected from the molecule while the incident electron has an appropriate energy left to become the orbital electron. Under the incidence of electrons with energy E_e, Gryzinski gave

$$Q_{\text{exch}}(E_e, U_n, U_{n+1}, U_i) = \frac{N_e \sigma_0}{U_n^2} \frac{U_{n+1} - U_n}{U_n} g_{\text{exch}},$$

where $\sigma_0 = 6.56 \times 10^{-14}$ eV^2 cm^2,

and

$$g_{\text{exch}} = \begin{cases} \frac{U_n^2}{(E_e+U_i)(E_e+U_i-U_n)} \times \frac{U_n}{U_i} \times \frac{E_e-U_n}{U_{n+1}-U_n} & \text{if } E_e \leqslant U_{n+1} \\ \frac{U_n^2}{(E_e+U_i)(E_e+U_i-U_n)} \times \frac{U_n}{E_e+U_i-U_n} & \text{if } E_e > U_{n+1} \end{cases} \tag{1}$$

N_e is the number of the equivalent electrons and U_i the ionization energy. The selection of U_n which is the minimum energy gain for an electron to be excited to the level n and U_{n+1} which is the energy to the next level $n+1$, is a little ambiguous (see refs [8,9]) and arbitrary for the molecules. Here we select U_n as the energy difference between the dissociation limit U_d and U_v, and U_{n+1} as the ionization energy of H_2 in the vth vibrational level of the ground state ([8] used a little different scheme).

The energy differential cross-section for the molecules can be expressed by

$$\frac{dQ_D}{dU_v} = q_{vv} Q_{\text{exch}}, \tag{2}$$

where q_{vv} is the Franck–Condon density, between vibrational level v in the Xstate and continuum energy level U_v in the repulsive state. It can be calculated by means of the δ function approximation [6–8].

$$q_{vv} = \left(\frac{dV(R)}{dR}\right)^{-1}_{R=R_{tp}} \psi_v^2(R_{tp}), \tag{3}$$

where ψ_v is the vth vibrational wave function in ground state and R_{tp} is the classical turning point of the repulsive state at energy level U_v.

For the cross-section at electron energy E_e, it can be calculated by the integration of Eq. (2) in the energy interval accessible, which is in our selection, between the dissociation limit U_d and the incident electron energy E_e plus the energy of vth vibrational level in the ground state, U_v. The integration range is a little different from [8].

For the energy distribution (f_{dis}) of the dissociated atoms, we assume when a molecule is projected to the repulsive state at an energy level U_v, it is immediately dissociated while the energy difference with the dissociation limit is equally shared by each atom. One can have,

$$f_{\text{dis}}(E_d, E_e) = V_e(E_e) \sum_{v=0}^{14} N_V \left(\frac{dQ_D}{dU_v}\right)_{U_v = 2E_d + U_d}. \tag{4}$$

$V_e(E_e)$ is the velocity of electrons and N_v is the vibrational distribution function. N_v was assumed here as a Maxwellian distribution characterized by so called vibrational temperature, T_{vib}. It was shown in [10] by the detailed consideration of the collision processes in multicusp plasmas, the vibrational distribution deviates from the Maxwellian and has a plateau regime in the middle vibrational levels. On the contrary, Fantz indicated in [11] and [12] that the Maxwellian might be a proper approximation for the vibrational distribution from the spectroscopic measurements and a modified collisional–radiative model calculation. In our recent experimental studies, we measured the Fulcher transition of H_2 in different discharge conditions, it seems to be that a dual Maxwellian fitting scheme gives a proper interpretation to the measured vibrational bands [13]. We adopt here the Maxwellian distribution for the vibrational population of H_2 in the ground state. Our evaluation of the vibrational distribution is underway.

When the incident electrons at a given energy distribution, i.e. for a Maxwellian distribution, one find,

$$f_{\text{dis}}(E_d, T_e) = \int_{E_{\text{th}}}^{\infty} \left(f_e(E_e) V_e^2(E_e) \sum_{v=0}^{14} N_V \left(\frac{dQ_D}{dU_v}\right)_{U_v = 2E_d + U_d} \right) dE_e, \tag{5}$$

where f_e is the electron distribution function.

We use FCFRKR code [14,15] for the calculation of the discrete wave functions and the molecular constants are adopted from [16]. The cross-sections calculated for the ground vibrational level are between the values reported in [6] and [8] in which the same method was used

for the calculations and good agreements with the existing experimental results and theoretical calculations were reported. The dependence of the cross-section on the vibrational level and the electronic energy is close to those reported in [6] and [8].

In Fig. 1(a), we reported the dependence of the energies of the dissociated products via the X–b transition on the vibrational distribution. The curvature characteristic of each curve is mainly due to the Franck–Condon densities. It is shown that when the vibrational temperature increases, namely, the molecules are vibtationally excited, the distribution of the dissociated atoms is shifted to the low energy part. When the vibrational temperature reaches about 1 eV, there is a significant distribution of dissociated atoms in the energy range less than 1 eV. However, the distribution in the high energy range ($E_d > 3$ eV), is relatively small. These phenomena for E_d can be easily understood by examining Fig. 2. When the molecules are at a higher vibrational level, the classical turning point of the electronic ground state at right side is shifted to longer inter atomic distance and the inverse gradient of the repulsive state is large at the same atomic separation. So the Franck–Condon density is larger at a lower continuum energy level of the repulsive state. Moreover, the dissociation energy is lower for a higher vibrational level so that the cross-section is higher when the impact electron energy is near the threshold. So, when the molecules are vibrationally excited, the dissociated atoms from the X–b transition are distributed highly in the low energy range. At higher continuum levels, one can see the gradient of the repulsive potential curve has larger value. So the overlap of the wave functions is small and thus the probability of the dissociated atoms in the high energy region is low.

In addition to the dissociation due to the direct excitation to the repulsive state, the excitation to $a^3\Sigma_g$ and $c^3\Pi u$ states may have considerable contributions to the dissociation. The $a^3\Sigma_g$ state can be radiatively related with the $b^3\Sigma_u$ state while the $c^3\Pi_u$ state is not radiatively related to the $b^3\Sigma_u$ state but it has only 0.05 eV energy difference with the state $a^3\Sigma_g$, so that $c^3\Pi_u$ may be easily transited to the state $a^3\Sigma_g$ and then radiatively decay to the $b^3\Sigma_u$ state. We calculated here the cross-sections of the reaction X → a again in the framework of Gryzinski approximation. The cross-section of the excitation X → a may be written as

$$Q^{a,v'}_{X,v} = q_{v,v'} Q_{\text{exch}}. \tag{6}$$

$q_{v,v'}$ is the Franck–Condon factor, where v and v' denote the vibrational levels of the ground state and $a^3\Sigma_g$, respectively. The cross-section of X–a–b can be written as

$$\frac{dQ^{X,v\to a\to b}_D}{dU_v} = \sum_0^{v'_{\max}} Q^{a,v'}_{X,v} \frac{A^{b,v}_{a,v'}}{A_{a,v'}}, \tag{7}$$

where $A^{b,v}_{a,v'}$ is the radiative transition probability of the (a, v') state to the (b, v) state and $A_{a,v'}$ is the total irradiation rate of the (b, v) state. Assuming the a–b transition is the only transition and adopting the electronic matrix moment has no dependence on the vibrational levels, then $A^{b,v}_{a,v'}/A_{a,v'}$ is reduced to be $\sim q^{a-b}_{v'v}(E_{a,v'} - U_v)^3$. The total cross-section and the energy distribution of the dissociated products can be obtained in an analogous way to the X–b transition.

Fig. 1(b) gives the energy distribution of the dissociated atoms via X–a–b and Fig. 1(c) via both X–b and X–a–b. Different from the X–b transition, one can see that for the dissociation via the channel X–a–b even at low vibrational temperature (0.1 eV), the dissociated atoms are mostly distributed in low energy (<1 eV). One can examine Eq. (7), the energy differential cross-section

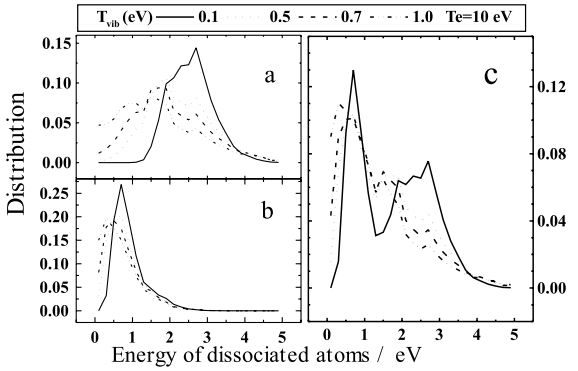

Fig. 1. The energy distribution of the dissociated products. (a) The dissociation from X-b, (b) from X–a–b, (c) from both X–b and X–a–b.

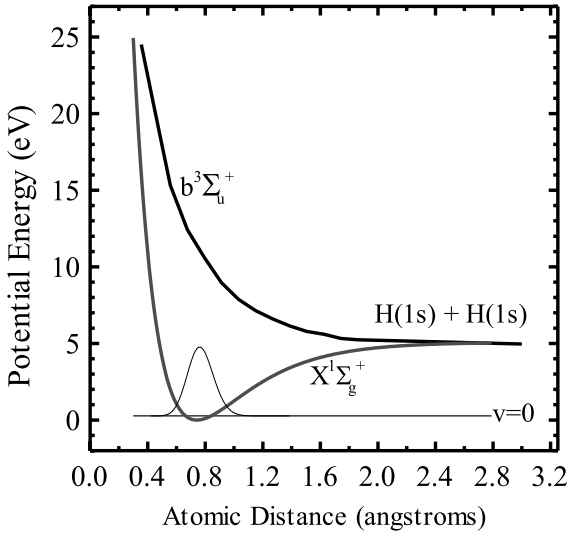

Fig. 2. The potential curves of the hydrogen molecules in $X^1\Sigma_g^+$ and $b^3\Sigma_u^+$ states.

has a cubic dependence on the energy difference between a vibrational level of $a^3\Sigma_g$ and a continuum energy level of $b^3\Sigma_u$. This gives rise to more dissociated atoms from X–a–b to be distributed in low energy than those from X–b.

3. Discussion

One would be interested in the contribution of the dissociated atoms to the Hα profiles. Therefore, one can apply the energy distribution of the dissociated atoms directly to the explanation of the experimental spectra, or to a modeling. However, through a DEGAS 2 [17] modeling and the comparison with the experiment [18] it was shown in [2] that in low temperature plasmas, i.e., plasmas in MAP device [18], H(2s) from the reaction channel

$$H_2(X^1\Sigma_g^+) + e \rightarrow H_2(1s\sigma, nl\lambda|^1\Lambda) \rightarrow e + H(1s) + H(2s) \quad \text{(reaction B)}$$

has the dominant contribution to the observed Hα spectra especially in the low energy range (<1 eV).

Here we show in Fig. 3, the contributions of Hα emission from dissociation of two important channels. One is reaction B indicated above. The other channel is reaction A.

In the electron temperature of ~10 eV and vibrational temperature of ~1 eV, the present calculation shows the reaction rates of reaction A is $\sim 6 \times 10^{-9}/\text{cm}^3$ which is lower than that in DEGAS 2 package ($8–9 \times 10^{-9}/\text{cm}^3$) and higher about a factor of 5 than that used in [2] for reaction B. Hα contributions from H(1s) and H(2s) from the reaction B differ by a factor of ~70. So even if we assume the energy of the dissociated atoms

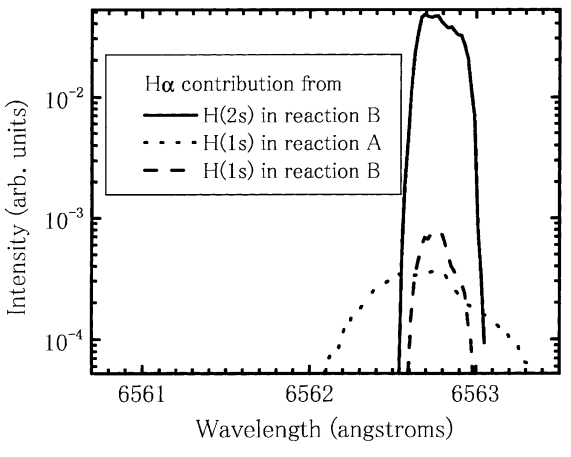

Fig. 3. The contributions of the dissociated atoms to Hα.

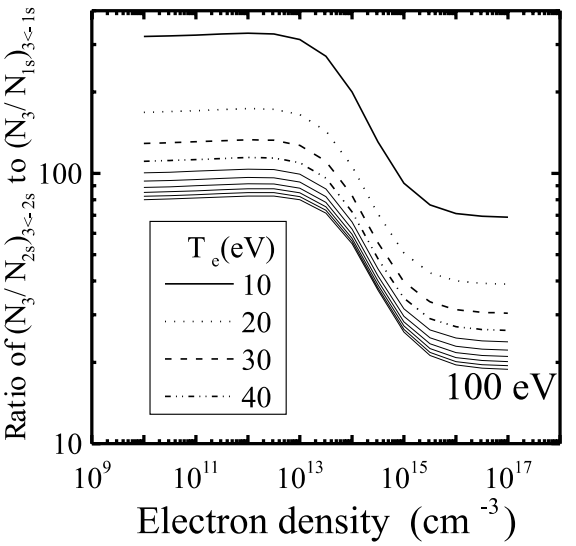

Fig. 4. The ratio of $n = 3$ populations due to the excitations of H(1s) and H(2s).

from the reaction A has the same energy as that held by the dissociated atoms (with the energy about 0.3 eV) from the reaction B, the Hα, contributions from this channel cannot exceed one tenth of that from reaction B. So we conclude that the dissociation from reaction A contributes insignificantly to Hα emission although it has largest dissociation rates in low temperature and low density plasmas.

The above discussion is valid in MAP plasmas characterized by the electron temperature of ~10 eV and the density of $3 \times 10^{11}/\text{cm}^3$. In this case, suppressed radiation of hydrogen atoms due to ionization is not effective. However, when electron temperature becomes higher to several 10 eVs and density becomes higher to over than $10^{14}/\text{cm}^3$, the Hα radiation due to the excitation of unit H(1s) will be considerably high to a few tenths of that due to unit H(2s) as one can see from Fig. 4 which shows the ratio of the population of $n = 3$ contributed from H(1s) to that from H(2s) when we use a minor revised scheme [2] of Fujimoto's C–R model [19]. In this case, the energy distribution of the dissociated atoms in the ground state will be reflected significantly on the Hα profiles.

4. Summary

We demonstrated the energy distribution of the dissociated products through the excitation the $b^3\Sigma_g$ and $a^3\Sigma_g$ states in the framework of the Gryzinski approximation. It was shown that the energy of the dissociated products of H_2 as well as the reaction rates has large

dependence on the vibrational distribution of the H_2 molecules. The dissociated products will be distributed toward low energy when molecules are highly excited. So these vibrational excited molecules may explain the low energy atoms observed in some devices. However, the contribution of Hα spectra especially in the low energy range (<1 eV) cannot be just explained from the ground state dissociated atoms at least in the cases where the H(2s) has considerable production rates from the dissociation of H_2.

The full understanding of the energy distribution of dissociation products requires the exact knowledge of the vibrational distribution and electron energy distribution. The other processes such as the dissociation from the ionized hydrogen molecules and from the excitation to the continuum part of stable states will become important when the electron temperature is higher. Certainly, the evaluation of the cross-sections for the most important dissociation processes is also one of the key issues. Our study of the vibrational excitation of hydrogen molecules is in progress.

Acknowledgements

This work was done under the support of JSPS fellowship and JSPS grant-in-aid.

References

[1] M. Gryzinski, Phys. Rev. 138 (2A) (1965) A305, A322, A366.
[2] S. Tanaka, B.J. Xiao, K. Kobayashi, M. Morita, Plasma Phys. Control Fus. 42 (2000) 1091.
[3] A. Pospieszczyk et al., J. Nucl. Mater. 266–269 (1999) 138.
[4] R.K. Janev et al., Elementary Processes in Hydrogen–Helium Plasmas, Springer Series on Atoms and Plasmas, Springer, Berlin, 1987.
[5] M. Capitelli, R. Celiberto, in: R.K. Janev (Ed.), Atomic and Molecular Processes in Fusion Edge Plasmas, Plenum, New York, 1995, pp. 195.
[6] M. Cacciatore, M. Capitelli, Chem. Phys. 55 (1981) 67.
[7] M. Cacciatore, M. Capittelli, M. Dillonardo, Chem. Phys. 34 (1978) 193.
[8] R. Celiberto et al., Chem. Phys. 133 (1989) 355.
[9] E. Bauer, D. Bartky, J. Chem. Phys. 43 (1965) 2466.
[10] C. Gorse, M. Capitelli, Chem. Phys. 93 (1985) 1.
[11] U. Fantz, B. Heger, Plasma Phys. Control Fus. 40 (1998) 2023.
[12] U. Fantz, B. Schalk, K. Behringer, New J. Phys. 2 (2000) 7.1.
[13] S. Kado, K. Kobayashi et al., in preparation.
[14] H. Telle, U. Telle, Comput. Phys. Com. 28 (1982) 1.
[15] Program aaor (FCFRKR), CPC program library.
[16] G. Herzberg, Molecular Spectra and Molecular Structure, Princeton, New Jersey, 1958.
[17] D. Stotler, C. Karney, Contrib. Plasma Phys. 34 (2/3) (1994) 392.
[18] K. Kobayashi, S. Ohtsu, S. Tanaka, J. Nucl. Mater. 266–269 (1999) 850.
[19] K. Sawada, T. Fujimoto, J. Appl. Phys. 78 (1995) 2913.